Supporting Information

Sokolova et al. 10.1073/pnas.1222321110

SI Text

S1. Materials

RTS 100 *Escherichia coli* HY kit was purchased from 5PRIME; α,ω-di-fluorescein PEG 8000 (150 mg/mL) was purchased from Chemicell. DyLight 550 staining kit was purchased from Thermo Fisher Scientific. Alexa Fluor 647 was purchased from Invitrogen. Recombinant enhanced GFP (eGFP) (1 mg/mL) was purchased from Cell Biolabs. Recombinant GFP (rGFP) (1 mg/mL) was purchased from Roche Applied Science. Sylgard 184 silicone elastomer kit polydimethylsiloxane (PDMS) was purchased from Dow Corning. Fluorinert FC-40 oil was purchased from Sigma-Aldrich. GFP-His (plasmid pRSET5d-GFPHis) was a gift from Kerstin Blank (Radboud University Nijmegen, Nijmegen, The Netherlands). Fast folding eGFP (deGFP) (plasmid pRSET5d-UTR1-eGFP-Del6-229: from plasmid pRSET5d-GFPHis, insertion of UTR1-eGFP-Del6-229 from pBEST-OR2-OR1-UTR1-eGFP-Del6-229-T500) was a gift from Vincent Noireaux and Jonghyeon Shin (University of Minnesota, Minneapolis, MN), and T7 RNA polymerase (50 units/μL) was purchased from New England Biolabs.

S2. Device and Setup Operation

Liquids were pumped using adjustable pumps (Harvard Apparatus; PHD 2000 infusion). Temperature in the device was controlled via Bipolar Temperature Controller (CL-100). Droplets were stabilized with 2% krytox–jeffamine ED-900–krytox surfactant dissolved in fluorinated oil FC-40.

S3. Data Acquisition and Analysis

The devices were mounted on the inverted microscope (Olympus IX81) equipped with a motorized stage (Prior; Optiscan II). Fluorescent images were taken with the sensitive EMCCD camera (iXon; Andor) using illumination from the mercury lamp or the laser. Analysis of images was done by ImageJ or home-written MATLAB routine.

S4. Device Fabrication

Devices were fabricated using soft photolithography. The first step required for microfluidic device fabrication is the mold fabrication. Photolithographic fabrication was used to fabricate microchannels. SU-8 negative photoresist (Micro Resist Technology) was used for fabrication purpose. The device fabrication started with creating a design in an AutoCAD program. A high-resolution commercial image setter then printed this design on a transparency (JD Photo Tools) (Fig. S1 *A*–*C*). This transparency served as the photomask in contact photolithography to produce a negative relief in photoresist on a silicon wafer substrate.

SU8-2025 photoresist is spin-coated on a round silicon wafer with 50-mm diameter (Si-Mat Silicon Materials). Spin coating parameters were optimized to achieve the desired film thickness. Subsequently, the sample was soft-baked for 1 min at 65 °C, 3 min at 95 °C, and 1 min at 65 °C to evaporate the solvent and densify the film. Then, the samples were exposed to UV light ($\lambda = 365$ nm) in the mask aligner (Karl Suss MJB 3 UV 300/400) for 21 s through the photomask. After exposure, the sample was post-baked for a time that depended on the thickness of the photoresist (1 min at 65 °C, 2 min at 95 °C, and 1 min at 65 °C). The samples were rinsed with developer solution (mr-Dev600; Micro Resist Technology) to remove the non–cross-linked regions. The resulting height of the channels was 25 μm. Thus, the fabrication of the SU-8 mask for drop production and storage chamber was accomplished on a silicon wafer. In a similar way, SU-8 masters for the reservoir channels were obtained with a thicker photoresist SU8-100 to achieve 175-μm–deep channels. Thus, depending on the design used in the mask, masters for droplet production and reservoir channels were obtained.

S5. Control of Microdroplet Contents Using Bilayer Device

Exploiting the permeability of PDMS membrane for small molecules allowed us to precisely control the volume and contents of the droplets (Fig. S1*F*). The bottom thin layer (40 μm) contains traps (1), where droplets are captured and stored. It is sealed on top with the PDMS membrane (15 μm), through which molecules are diffused.

The top thick layer (5 mm) contains flow channels for flushing Milli-Q or a saturated salt solution. Each droplet stored in traps in the bottom layer is in contact with the top layer through a dialysis membrane. It is permeable to water and low–molecular-weight organic solvents. Using the semipermeable membrane, the solvent conditions in the droplets can be changed by changing ionic strength of the liquid flushing in the reservoir channels. Because transport through the dialysis membrane is a diffusion process, reducing the relevant dimensions 10-fold, will give a decrease in the typical time required for transport by a factor of 100.

Liquids that were flushed through the top layer of our devices were first flushed through a Peltier temperature control element (Warner Instruments), to assure accurate control over the temperature of the droplets (Peltier outflow temperature, ±0.5 °C; trap layer temperature, ±3 °C). See ref. 2 for a similar device setup.

S6. Method for mRNA Production Experiments in Cell Lysate

The reaction mixture contained the following: 10 μL of reaction mix, 5 μL of reconstitution buffer, 12 μL of amino acids, 1 μL of methionine, 12 μL of *E. coli* lysate, 10 μL of pRSET5d-GFPHis, and 1 μL of molecular beacon (1 μM) (*SI Text*, *S8*).

Droplets were produced in the double-layer device (oil flow: 120 μL/h; mixture flow: 30 μL/h). Constant temperature was maintained by flushing liquids through Peltier unit at the high flow rate of 100–500 μL/min. One part of the device was covered with channels containing Milli-Q, and the other part, with saturated salt solution at 4 °C. When phase separation had occurred in the droplets that were covered with salt-rich reservoir channels and distribution of all macromolecules (including DNA) over the two phases had reached equilibrium, the temperature of the device was raised to 25 °C (within a minute) to start up the reaction and followed the next 2 h using fluorescence microscopy. Device was mounted on Olympus IX81 inverted microscope, where sample was excited using mercury lamp. Fluorescence readout was performed using Andor iXon3 EMCCD. Calibration curve with the same acquisition settings for Alexa Fluor 647 was made to obtain concentrations of mRNA in the droplets (Fig. S2*A*).

S7. Method for GFP Production Experiments in Cell Lysate

The reaction mixture contained the following: 10 μL of reaction mix, 5 μL of reconstitution buffer, 12 μL of amino acids, 1 μL of methionine, 12 μL of *E. coli* lysate, and 10 μL of pRSET5d-UTR1-eGFP-Del6-229.

Droplets were produced in the double-layer device (oil flow: 120 μL/h; cell lysate flow: 30 μL/h). Constant temperature was

maintained by flushing liquids through Peltier unit at the high flow rate of 100–500 μL/min. One part of the device was covered with channels containing Milli-Q, and the other part, with saturated salt solution at 4 °C. When phase separation had occurred in the droplets that were covered with salt-rich reservoir channels and distribution of all macromolecules (including DNA) over the two phases had reached equilibrium, the temperature of the device was raised to 25 °C (within a minute) to start up the reaction and followed the next 2 h using fluorescence microscopy. The device was mounted on Olympus IX81 confocal microscope, where the sample was excited using 20% laser power (λ = 488 nm). Fluorescence readout was performed using an Andor iXon3 EMCCD camera at an exposure time of 0.1 s. Calibration curve with the same acquisition settings for eGFP was made to obtain concentrations of the protein in the droplets (Fig. S2*B*).

S8. Molecular Beacon for mRNA Production

The sequence of the molecular beacon used to probe the GFP mRNA (*SI Text*, *S6*) concentration was as follows: 5′-(Alexa 647)-GCGCAAAUAAAUUUAAGGGUAAGCGC-(Iowa Black Quencher)-3′. The backbone of the molecular beacon was composed of 2′-*O*-methylribonucleotides.

The molecular beacon was designed using the mfold program (3) according to the method of Bratu et al. (4), and by using the IntaRNA, version 1.2.5, program, accessible on the Freiburg RNA Tools server (http://rna.informatik.uni-freiburg.de:8080/IntaRNA.jsp).

The molecular beacon was synthesized by Integrated DNA Technologies (optical density at 260 nm = 5.3), resuspended in autoclaved Milli-Q water to a concentration of 50.2 μM, and stored in light-protected tubes at −20 °C.

S9. Home-Made in Vitro Transcription Translation System

Reaction mixtures of the home-made in vitro transcription translation kit were composed of one-third cell lysate and two-thirds reaction buffer. Both were prepared with slight modifications according to Shin and Noireaux (5). The lysate was prepared with *E. coli* BL21 cells grown at 37 °C in 2YT medium up to OD_{600} = 1.5. After cell growth, all further lysate purification steps were performed on ice or at 4 °C. The cells with a typical wet weight of 5 g were resuspended in 15 mL of S30 buffer A containing the following: 50 mM Tris, 60 mM potassium glutamate, 14 mM magnesium glutamate, 2 mM DTT, adjusted to pH 7.7, and centrifuged (3,000 × *g* for 10 min) twice. After a third resuspension with 5 mL of S30 buffer A, the cells were broken with a bead-beater (Biospecs Products; mini bead-beater-1) using 0.1-mm glass beads, followed by centrifugation (30,000 × *g* for 30 min). The supernatant was dialyzed with S30 buffer B (5 mM Tris, 60 mM potassium glutamate, 14 mM magnesium glutamate, pH 8.2, 1 mM DTT) for three times 45 min followed by one dialysis overnight (4× 250 mL) at 4 °C. A concentration of 22 mg/mL of proteins in the cell lysate was obtained, and the lysate was stored at −80 °C.

The reaction buffer consisted of 50 mM Hepes adjusted to pH 7.5, 1.5 mM ATP and GTP each, 0.9 mM CTP and UTP each, 1 mM spermidine, 0.75 mM cAMP, 0.33 mM NAD, 0.26 mM coenzyme A, 30 mM 3-phosphoglyceric acid (3-PGA), 0.068 mM folinic acid, 0.2 mg/mL tRNA, 1 mM isopropyl-beta-D-thiogalactopyranoside (IPTG), 1.5 mM of each amino acid, 20 mM magnesium glutamate, and 200 mM potassium glutamate and PEG 8000 [2% (wt/vol)]. Home-made T7 RNA polymerase was added to the final reaction mixture.

S10. Phase Separation of Cell-Free Expression Kit Containing Fluorescent PEG and Lysate

The reaction mixture contained the following: 10 μL of reaction mix, 5 μL of reconstitution buffer, 12 μL of amino acids, 1 μL of methionine, 12 μL of DyLight 550-stained *E. coli* lysate, 0.3 μL of 150 mg/mL α,ω-di-fluorescein PEG 8000, and 9.7 μL of Milli-Q.

Commercial lysate was stained using DyLight 550 NHS ester kit following the manufacturer's protocol.

The final sample volume was 50 μL with a total PEG concentration of 20.9 g/L. Droplets were generated in a double-layer device (oil flow: 120 μL/h; sample flow: 30 μL/h; 6 M NaCl solution: 100 μL/h) and observed for 2 h by fluorescence microscopy.

The fluorescence intensity was calculated using ImageJ, measuring the area, integrated density, and mean gray value (6). Radii and volumes of droplets and coacervates were calculated from the measured area. The corrected fluorescence intensity (F_{corr}) was calculated as follows:

$$F_{corr} = \iint_A f \, dx \, dy \; - A \, \overline{f_b}, \qquad [S1]$$

where f is the measured fluorescence intensity, $\overline{f_b}$ is the mean background fluorescence intensity, A is the cross-sectional area of the fluorescent droplet, and F_{corr} is the background-corrected integrated fluorescence intensity, which is proportional to the total amount of fluorescent molecules.

The volume and F_{corr} values of the PEG-poor phase were calculated by subtracting the coacervate values from the total droplet values. The ratio between the F_{corr} values (normalized to volume) of the PEG-rich and PEG-poor phase provided the partition coefficient P:

$$[\mathrm{PEG}]_{coac} = P \times \frac{V_0}{V_{coac}} \times [\mathrm{PEG}]_0, \qquad [S2]$$

where V is the volume and the subscripts 0 and coac denote the initial droplet and the coacervate phase, respectively.

The lysate partition coefficient and final lysate concentrations were calculated identically. Images were processed by adjusting the brightness/contrast in Photoshop CS 5.1. False color images were generated by applying a linear gradient map in Photoshop CS 5.1. An image stack was converted to an AVI movie using ImageJ.

The distribution of the macromolecular components over the two coexisting phases in our cell-free expression kit was studied in detail using a lysate containing both proteins that were covalently labeled with DyLight 550 and a small amount of α,ω-di-fluorescein–labeled PEG 8000. Droplets were generated in the same double-layer devices as described in *SI Text*, *S6* and *SI Text*, *S7*, and monitored for 2 h.

The partition percentages of PEG and lysate proteins were determined using the calculated F_{corr} and volume ratios between initial droplets and coacervates (Table S1). Droplet shrinkage induces the phase separation of PEG-rich droplets at a total internal salt concentration of 1.9 M and total PEG concentration (fluorescent and nonfluorescent) of 80 g/L. These small droplets fuse to form a PEG-rich coacervate which is ∼20-fold smaller in volume than the initial droplet (Movie S1). The (fluorescent) cell lysate accumulated into the coacervate as demonstrated by the rapid DyLight 550 fluorescence increase in the coacervate. Eventually, 75% of the proteins from the lysate and 78% of the PEG accumulated in the PEG-rich coacervate phase, corresponding to concentrations of 85 g/L proteins and 290 g/L PEG. The dilute phase contained 12 g/L proteins and 33 g/L PEG 8000.

S11. Phase Separation of Cell-Free Expression Kit Containing Lysate and rGFP

The reaction mixture contained the following: 10 μL of reaction mix, 5 μL of reconstitution buffer, 12 μL of amino acids, 1 μL of methionine, 12 μL of *E. coli* lysate, and 10 μL of rGFP 200 [nM].

rGFP (1 mg/mL) was added to the reaction mixture of commercial lysate (no plasmid was added). The fluorescence intensity, radii, and volumes of droplets and coacervates were calculated from the measured area according to the procedure described in *SI Text*, *S10*. Eventually 81% of rGFP accumulated in the coacervate (Fig. S3*B*).

S12. Phase Separation of PEG in the Absence of Cell-Free Expression Kit

The reaction mixture contained the following: 11.7 μL of 428 mM Hepes, pH 8.0; 10 μL of 1.5 mg/mL α,ω-di-fluorescein PEG 8000; 8 μL of 250 mg/mL PEG 8000; 3 μL of 5 M potassium glutamate; 3 μL of 500 mM magnesium glutamate; and 14.3 μL of Milli-Q.

The final sample volume was 50 μL with a total PEG concentration of 40.3 g/L. Droplets were generated in a single-layer device (oil flow: 120 μL/h; sample flow: 30 μL/h) and observed for 3 h by bright-field and fluorescence microscopy.

The area of the droplets was determined using ImageJ. Droplet radii and volumes were calculated from the measured areas. The volume ratio between the size of the initial droplet and the droplet size when phase separation occurs was used to calculate critical PEG and internal salt concentrations.

A mixture of Hepes buffer (100 mM, pH 8.0), PEG 8000 (40 g/L), α,ω-di-fluorescein PEG 8000 (0.3 g/L), potassium glutamate (300 mM), and magnesium glutamate (30 mM) was analyzed to investigate whether salt-induced phase separation of PEG 8000 can occur in the absence of components from the cell-free expression kit. Potassium glutamate and magnesium glutamate were used as they are the main salts present in most cell-free protein expression mixtures (5). Droplets were generated in single-layer devices and evaporation-induced droplet shrinkage was followed for 3 h. Upon shrinking, the mixture phase separated into a highly fluorescent PEG-rich phase and a nonfluorescent phase (Fig. S3 *C* and *D*). The PEG-rich phase strongly localizes to the droplet/oil interface, either appearing as bright circles when localized to the top or bottom of the droplet or crescent moon shaped when localized to the sides. The ratio between the initial droplet volume and the volume of shrunk droplets where phase separation occurred showed that the mixture undergoes phase separation at ∼180 g/L PEG 8000 and an internal ionic strength of 1.9 M.

S13. Inductively Coupled Plasma Optical Emission Spectrometry

The total K, Na, Mg, Zn, P, and S content of the cell-free expression kit, the coacervates, and the dilute phase coexisting with the coacervates was determined by inductively coupled plasma-optical emission spectrometry (ICP-OES) (Thermo Scientific; iCAP 6300). We prepared five samples of reaction mixture (50-μL total volume) in small volume Eppendorf tubes, as described in *SI Text*, *S7*. One of these samples was kept at 4 °C and used for the analysis of the reaction mixture before phase separation. The other four samples were brought to phase separation by evaporating part of the water under a constant flow of argon at 4 °C. We measured the mass of all samples before and after phase separation. A small volume (2–5 μL) of the coacervate (bottom) and dilute (top) phase was taken from each Eppendorf tube and transferred to a new Eppendorf. Then, 100 μL of concentrated nitric acid (HNO_3, 65%) was added on top of these ICP samples and the total volume was transferred quantitatively into Milli-Q [total volume, 5.0 mL; final nitric acid concentration, 1.3% (vol/vol)] in polystyrene sample tubes. To the non–phase-separated sample, we added 100 μL of concentrated nitric acid as well, and then transferred it to Milli-Q (total volume, 5.0 mL) quantitatively.

ICP-OES analysis was carried out for K, Na, Mg, Zn, P, and S. The instrument was calibrated using one blank and four standards of known concentration of K, Na, Mg, Zn, P, and S in Milli-Q. The detection limit for each element was 1 ppm or lower. Table S2 summarizes the resulting concentrations of K, Na, Mg, Zn, P, and S in the coacervates, the dilute phase, and in the cell-free expression kit before phase separation.

S14. Covalent Labeling of the Plasmid

Plasmids were covalently labeled with fluorescein using the Label IT Tracker Intracellular Nucleic Acid Localization Kit, Fluorescein from Mirus Bio. The following protocol was used: 5 μL of 10× labeling buffer A. 8 μL of Label IT Tracker reagent, 6.3 μL of pIVEX GFP plasmid (1,263.9 ng/μL), and 30.7 μL of Milli-Q.

The reaction mixture was incubated for 1 h at 37 °C. After addition of 0.1 vol of 5 M NaCl and 2 vol of ice-cold 100% ethanol, the sample was incubated overnight at −20 °C.

The labeled plasmid was pelleted by centrifugation at 14,000 × *g* for 10 min, followed by a washing step by centrifugation at 14,000 × *g* for 10 min with 0.5 mL of 70% ethanol to remove residual salts. The pellet was dissolved in 50 μL of Milli-Q.

Plasmid concentration and labeling density were determined by UV-visible spectrophotometry. The final plasmid concentration was 145 ng/μL, and the plasmid was labeled with a fluorescein every 336 bases on average.

For the plasmid localization experiment, the reaction mixture contained the following: 10 μL of reaction mix, 5 μL of reconstitution buffer, 12 μL of amino acids, 1 μL of methionine, 12 μL of *E. coli* lysate, and 10 μL of labeled pIVEX plasmid (145 ng/μL).

The sample was prepared and imaged as described in *SI Text*, *S7*, but kept at 4 °C. Fluorescence readout was performed using Andor iXon EMCCD camera using an exposure time of 0.5 s. Plasmid partitioning was determined as described in *SI Text*, *S10*.

S15. Fluorescence Recovery After Photobleaching

Photobleaching experiments were performed on an Olympus IX81 confocal microscope, equipped with an Andor iXon3 camera, Andor 400-series solid-state lasers, a Yokogawa CSU-X1 spinning disk, and an Andor FRAPPA photobleach module. Microdroplets of cell lysate, to which 200 nM eGFP (Cell Biolabs) was added, were bleached before and after phase separation at 100% laser intensity (λ = 488 nm), using three subsequent pulses of 20 μs. For bleaching, a thin stripe was selected in the middle of the droplet or the coacervate, such that the intensity profile perpendicular to the stripe, across the droplet was symmetric. Recovery of the fluorescence intensity was monitored at a fivefold reduced laser intensity (λ = 488 nm), using an exposure time of 15 ms. Taking into account the readout time, the imaging frequency was 1/51 ms^{-1} or 1/105 ms^{-1} for droplets before and after phase separation, respectively.

For the analysis of the fluorescence images, we use a custom-made routine in MATLAB. Following Elowitz et al. (7) and Konopka et al. (8), we consider the recovery of the spatial eGFP concentration distribution to be a one-dimensional diffusion problem. We assume that the concentration c of eGFP is proportional to the fluorescence intensity f. At every slice perpendicular to the bleaching stripe, the equation governing the diffusion of eGFP can be written as follows:

$$\frac{\partial c}{\partial t} = D\frac{\partial^2 c}{\partial x^2}, \qquad \textbf{[S3]}$$

where the droplet edges are located at $x = 0$ and $x = b$. At the boundaries, reflecting boundary conditions apply

$$\left.\frac{\partial c}{\partial x}\right|_{x=0} = 0 \qquad \left.\frac{\partial c}{\partial x}\right|_{x=b} = 0. \qquad \textbf{[S4]}$$

The general solution to this equation can be written as a Fourier series:

$$c(x,t) = \sum_{n=0}^{\infty} A_n \cos\left(\frac{n\pi x}{b}\right) \exp\left(-\frac{Dn^2\pi^2 t}{b^2}\right). \qquad \textbf{[S5]}$$

We assume the initial bleached profile can be written as a step function

$$c(x,0) = c_b + (c_0 - c_b)\left(H\left(x - \frac{b}{2} - a\right) + H\left(\frac{b}{2} - a - x\right)\right), \qquad \textbf{[S6]}$$

where c_0 is the uniform concentration of eGFP in the droplet before bleaching and c_b is the concentration of eGFP in the bleached area, directly after bleaching. $H(z)$ denotes the Heaviside step function. The amplitudes of the Fourier series solution can be written as follows:

$$\begin{aligned} A_n &= \frac{2}{b}\int_0^b c(x,0)\cos\left(\frac{n\pi x}{b}\right) \mathrm{d}x \\ &= c_0 - \frac{2a(c_0 - c_b)}{b} + \sum_{n=1}^{\infty} \frac{2(c_0 - c_b)}{n\pi}\left[\sin\left(\frac{n\pi(b-2a)}{2b}\right)\right. \\ &\quad \left. - \sin\left(\frac{n\pi(b+2a)}{2b}\right)\right]. \end{aligned} \qquad \textbf{[S7]}$$

Finally, the recovery profile follows from integration over the bleached area as follows:

$$F(y,t) = \int_{b/2-a}^{b/2+a} f(x,y,t)\ \mathrm{d}x. \qquad \textbf{[S8]}$$

The experimental fluorescence recovery F was calculated from the time-dependent confocal microscope images of bleached droplets. For every image, a background intensity, measured far outside the droplet, was subtracted from the fluorescence intensity, and the net fluorescence intensity was integrated over the bleached area in x direction, and averaged over 10–20 y slices. The experimental recovery data were fitted to the predicted recovery based on the Fourier series solution, with fixed values for a, b, c_0, and c_b that were taken from the images and using the diffusion coefficient D as a fitting parameter. The results of our analysis are described in the main text.

S16. Modeling of Transcription and Translation in Cell Lysate

We constructed a deterministic model of transcription and translation in the cell-free expression kit, based on the underlying biochemical reactions, using a similar framework as outlined by Karzbrun et al. (9), Stögbauer et al. (10), and Stricker et al. (11). Both transcription (TS) and translation (TL) occur in two steps. First, a rapid-equilibrium binding of the enzyme (T7 RNA polymerase or the ribosomal complex) and the template molecule (DNA or mRNA, respectively) is established as follows:

$$\mathrm{DNA} + \mathrm{Pol} \underset{k_r}{\overset{k_f}{\rightleftarrows}} \mathrm{DNA-Pol}, \qquad \textbf{[S9]}$$

where the equilibrium constant $K_{TS} = k_f/k_r = [\mathrm{DNA-Pol}]/([\mathrm{DNA}] \times [\mathrm{Pol}])$, or equivalently, $K_{TL} = [\mathrm{mRNA-Rib}]/([\mathrm{mRNA}] \times [\mathrm{Rib}])$, and [A] denotes the actual concentration of free A. The complex, DNA-Pol or mRNA-Rib, then produces mRNA and protein, respectively, at an overall catalysis rate as follows:

$$\frac{\mathrm{d}[\mathrm{mRNA}]}{\mathrm{d}t} = k_{TS} \times [\mathrm{DNA-Pol}] - k_{XS} \times [\mathrm{mRNA}], \qquad \textbf{[S10]}$$

where k_{TS} (k_{TL}) is the catalysis rate constant of transcription (translation), which can be converted into an effective rate of nucleotide incorporation or amino acid incorporation, if the length of the mRNA and GFP is known. The actual concentration of complex is obtained as the real, positive root of the quadratic equation derived from Eq. **S9**.

$$K_{TS}[X]^2 - (K_{TS}\, c_{DNA} + K_{TS}\, c_{Pol} + 1)[X] + K_{TS}\, c_{DNA}\, c_{Pol} = 0, \qquad \textbf{[S11]}$$

where c_A denotes the overall concentration of component A and X is the complex DNA-Pol.

The incorporation of nucleotides into the growing mRNA consumes NTPs. The incorporation of amino acids into the growing GFP consumes two GTPs and one ATP per amino acid. To account for the slowdown of transcription and translation due to depletion of NTPs and amino acids, we add normalized prefactors containing [NTP] and [aa] to Eq. **S10** and the equivalent expression for translation.

Eq. **S10** also contains a degradation term of mRNA by RNase with rate constant k_{XS} (k_{XL} for protein degradation by proteases in translation). We find that the rate of both degradation processes can be neglected in the commercial cell-free expression kit on the timescale of the expression experiments in droplets (Fig. S5 *A* and *B*), in contrast to the model used by Karzbrun et al. (9), and we have used $k_{XS} = k_{XL} = 0$ and $[\mathrm{RNAse}] = [\mathrm{protease}] = 0$ in all model calculations.

After production of the protein, an additional, first-order maturation (folding) step can be included, with maturation rate constant k_{mat}, leading to the maturated, fluorescent GFP* or deGFP*. For studies on deGFP production, we use a fixed maturation rate constant of $k_{mat} = 1/8.5 \quad \mathrm{min}^{-1}$ (5).

Finally, an overall inactivation of the transcription and translation machinery could account for the fact that mRNA and protein production levels off at a constant point in time (100–120 min after start), independent of DNA concentration and independent of the amount of protein produced, as was argued by Stögbauer et al. (10). The exact origin of this inactivation process is not fully understood yet. Following Stögbauer et al., we include a first-order inactivation of the transcription and translation machinery, governed by an inactivation constant k_{iTS} (k_{iTL}).

In summary, our model contains the components DNA, mRNA, GFP, GFP*, Pol, Rib, $\mathrm{NTP_{C/U}}$, $\mathrm{NTP_{A/G}}$, and aa, and constants K_{TS}, K_{TL}, k_{TS}, k_{TL}, k_{mat}, k_{iTS}, and k_{iTL}, and the time evolution of these components can be described using the following set of differential equations:

$$\frac{d[mRNA]}{dt} = k_{TS}\ \alpha_{NTP}\ [DNA-Pol] - k_{XS}\ [mRNA] \quad \textbf{[S12]}$$

$$\frac{d[GFP]}{dt} = k_{TL}\ \alpha_{NTP}\ \alpha_{aa}\ [mRNA-Rib] - k_{mat}\ [GFP] - k_{XL}\ [GFP] \quad \textbf{[S13]}$$

$$\frac{d[GFP^*]}{dt} = k_{mat}\ [GFP] - k_{XL}\ [GFP^*] \quad \textbf{[S14]}$$

$$\frac{d[NTP]_{U/C}}{dt} = -\frac{k_{TS}\ L_{mRNA}\ \alpha_{NTP}}{2} \times [DNA-Pol] \quad \textbf{[S15]}$$

$$\frac{d[NTP]_{A/G}}{dt} = -\frac{k_{TS}\ L_{mRNA}\ \alpha_{NTP}}{2} \times [DNA-Pol] - 2k_{TL}\ L_{GFP}\ \alpha_{NTP}\ \alpha_{aa} \times [mRNA-Rib] \quad \textbf{[S16]}$$

$$\frac{d[aa]}{dt} = -2k_{TL}\ L_{GFP}\ \alpha_{NTP}\ \alpha_{aa} \times [mRNA-Rib] + k_{XL}\ L_{GFP} \times ([GFP]+[GFP^*]) \quad \textbf{[S17]}$$

$$\frac{d[Pol]}{dt} = -k_{iTS} \times ([Pol]+[DNA-Pol]) \quad \textbf{[S18]}$$

$$\frac{d[Rib]}{dt} = -k_{iTL} \times ([Rib]+[mRNA-Rib]). \quad \textbf{[S19]}$$

The actual concentrations of the complexes DNA-Pol and mRNA-Rib are obtained from Eq. **S11**. The prefactors α_{NTP} and α_{aa} indicate the overall remaining amount of nucleotides and amino acids relative to their initial concentrations (a fraction). The lengths of mRNA (L_{mRNA}) and GFP (L_{GFP}) are taken to be 3×238 and 238, respectively.

We solve the above set of differential equations for a given set of initial concentrations and rate constants using MATLAB. We have chosen the binding constants relevant for transcription and translation the same as reported previously (10). Briefly, for single-phase droplets, $K_{TS} = 0.12$ nM^{-1}, $K_{TL} = 0.015$ nM^{-1}, $k_{TS} = 25$ min^{-1}, $k_{TL} = 0.80$ min^{-1}, $k_{mat} = 0.12$ min^{-1}, $k_{iTS} = 0.02$ min^{-1}, and $k_{iTL} = 0.1$ min^{-1}. For phase-separated droplets, $K_{TS} = 10^0 - 10^2$ nM^{-1}, $K_{TL} = 0.015$ nM^{-1}, $k_{TS} = 143$ min^{-1}, $k_{TL} = 0.12$ min^{-1}, $k_{mat} = 0.12$ min^{-1}, and $k_{iTS} = 0.5$ min^{-1} and $k_{iTL} = 0.1$ min^{-1}.

The initial concentrations of NTPs, T7 RNA polymerase, and ribosomes were estimated from our fits, in combination with a comparison with experiments with our home-made cell-free expression kit, yielding $c_{Pol} = 4.1$ nM, $c_{Rib} = 16$ nM, $c_{UTP} = c_{CTP} = 0.28$ mM, $c_{ATP} = c_{GTP} = 0.81$ mM, and $c_{aa} = 1.0$ mM for all amino acids. We corrected all concentrations for the actual droplet and coacervate sizes after shrinkage and phase separation (Table S1), thereby also taking into account the partitioning coefficients of DNA, proteins, and salt, as described in *SI Text*, *S10–S14*.

The DNA concentration can be varied by changing the amount of plasmid stock solution that is added to the reaction mixture (*SI Text*, *S6*). However, we found that a small amount of DNA adsorbs to the oil–water interface (Fig. S4 *A* and *B*). We corrected the DNA concentration in the models for this adsorption, by subtracting a fixed amount of DNA from the concentration in the initial droplet, before distributing it over the coacervate and the dilute phase (with a partitioning coefficient as determined following the method in *SI Text*, *S14*). We keep this fixed adsorbed amount in the model constant for all experiments and found that an adsorbed amount of 0.095 μm^{-2}, corresponding to a concentration of 35 pM in a reference droplet of 27-μm diameter, is in good agreement with our experimental data, because we find that mRNA production is strongly suppressed in droplets containing as little as 40 pM DNA (Fig. S6*E*).

The binding constants (K) and rate constants (k) of the transcription and translation in the commercial cell-free expression kit in microdroplets, before and after phase separation, were obtained from fits of our data to the individual solutions of the above set of differential equations. We reported these values in the main text and in Figs. S1–S6.

In the case of mRNA production, all data points measured after droplet formation were shifted by a fixed delay time, which is a direct result of the time needed to heat up the samples from 4 °C to 25 °C. The delay time is found by requiring that the steepest slope, expressed as $\Delta[mRNA]/\Delta t$, measured over at least three subsequent points, was located at $t = 0$. This approach is analogous to the approach by Karzbrun et al. (9), who denote this delay time τ_0. In the case of protein production, all data points were shifted by the same fixed delay time as for mRNA production and no additional protein production delay τ_f was included.

Finally, the mRNA concentrations and mRNA fits that are reported in the main text and in Figs. S1–S6 for different initial DNA concentrations are (re)normalized using a reference droplet of 27-μm diameter and a coacervate of 13-μm diameter, to allow qualitative comparison of the mRNA production rates.

S17. Method for Transcription in Bulk at Various PEG Concentrations

See Fig. S5*C*.

The reaction mixture contained the following: Tris·HCl, pH 8.1, 40 mM; DTT, 5 mM; spermidine, 1 mM; $MgCl_2$, 25 mM; ATP, GTP, CTP, UTP, 4 mM each; guanosine monophosphate, 5 mM; T7 RNA polymerase, 1 unit/μL of reaction mixture; PEG 8000 concentrations of 0%, 2%, 5%, 8%, 10%, 11.5%, and 16.5%; and 3 nM pRSET5d-GFPHis.

The reaction was run at 30 °C for 3 h and analyzed on a 8% acrylamide gel (TBE buffer, 8 M urea).

See Fig. S5*D*.

The reaction mixture contained the following: Tris·HCl, pH 8.1, 40 mM; DTT, 5 mM; spermidine, 1 mM; $MgCl_2$, 25 mM; ATP, GTP, CTP, and UTP, 4 mM each; guanosine monophosphate, 5 mM; T7 RNA polymerase, 1 unit/μL of reaction mixture; PEG 8000 concentrations of 0%, 2%, 5%, 8%, 10%, 11.5%, and 16.5%; pRSET5d-GFPHis, 3 nM for low- and 1 nM for high-salt experiments; and 1 μL of molecular beacon (1 μM) (*SI Text*, *S8*). K^+ was brought to 975 mM (equal to the salt concentration inside the coacervates; see *SI Text*, *S13*) by addition of solid potassium glutamate before incubation.

Transcription in bulk was followed by fluorescence measurements in a microplate (Nunclon 96 Flat Bottom Black Polystyro), using a microplate reader (Tecan Infinite 200Pro) with excitation $\lambda = 630$ nm and emission $\lambda = 667$ nm. The reaction was carried out at 30 °C and followed for the next 4 h.

See Fig. S5*F*.

The home-made in vitro transcription and translation system was prepared as described in *SI Text*, *S9* with pRSET5d-GFPHis (1 nM) and PEG 8000, 2%, 5%, 8%, and 10% (wt/vol). Before incubation, 1 μL of molecular beacon (*SI Text*, *S8*) was added to the reaction mixture to allow detection of mRNA. In addition, solid potassium glutamate was added to reach a final K^+ concentration of 975 mM (equal to the potassium concentration inside the coacervates; see *SI Text*, *S13*).

Transcription in bulk was followed by fluorescence measurements on a microplate reader (same as above) with excitation $\lambda = 630$ nm and emission $\lambda = 667$ nm. The reaction was carried out at 30 °C and followed for the next 4 h.

S18. Method for Translation in Bulk at Various PEG Concentrations

See Fig. S5*E*.

The home-made in vitro transcription and translation system was prepared as described in *SI Text*, *S9*. With pRSET5d-GFPHis (5 nM) and PEG 8000, 2%, 4%, 7%, and 10% (wt/vol). Translation in bulk was followed by fluorescence measurements in a microplate (Nunclon 96 Flat Bottom Black Polystyro), using a microplate reader (Tecan Infinite 200Pro) with excitation $\lambda = 395$ nm and emission $\lambda = 509$ nm. The reaction was carried out at 37 °C and followed for the next 5 h.

1. Schmitz CHJ, Rowat AC, Köster S, Weitz DA (2009) Dropspots: A picoliter array in a microfluidic device. *Lab Chip* 9(1):44–49.
2. Velve Casquillas G, et al. (2011) Fast microfluidic temperature control for high resolution live cell imaging. *Lab Chip* 11(3):484–489.
3. Zuker M (2003) Mfold web server for nucleic acid folding and hybridization prediction. *Nucleic Acids Res* 31(13):3406–3415.
4. Bratu DP, Catrina IE, Marras SAE (2011) Tiny molecular beacons for in vivo mRNA detection. *Methods Mol Biol* 714:141–157.
5. Shin J, Noireaux V (2010) Efficient cell-free expression with the endogenous *E. coli* RNA polymerase and sigma factor 70. *J Biol Eng* 4:8.
6. Potapova TA, Sivakumar S, Flynn JN, Li R, Gorbsky GJ (2011) Mitotic progression becomes irreversible in prometaphase and collapses when Wee1 and Cdc25 are inhibited. *Mol Biol Cell* 22(8):1191–1206.
7. Elowitz MB, Surette MG, Wolf PE, Stock JB, Leibler S (1999) Protein mobility in the cytoplasm of *Escherichia coli*. *J Bacteriol* 181(1):197–203.
8. Konopka MC, Shkel IA, Cayley S, Record MT, Weisshaar JC (2006) Crowding and confinement effects on protein diffusion in vivo. *J Bacteriol* 188(17):6115–6123.
9. Karzbrun E, Shin J, Bar-Ziv RH, Noireaux V (2011) Coarse-grained dynamics of protein synthesis in a cell-free system. *Phys Rev Lett* 106(4):048104–048108.
10. Stögbauer T, Windhager L, Zimmer R, Rädler JO (2012) Experiment and mathematical modeling of gene expression dynamics in a cell-free system. *Integr Biol (Camb)* 4(5):494–501.
11. Stricker J, et al. (2008) A fast, robust and tunable synthetic gene oscillator. *Nature* 456(7221):516–519.

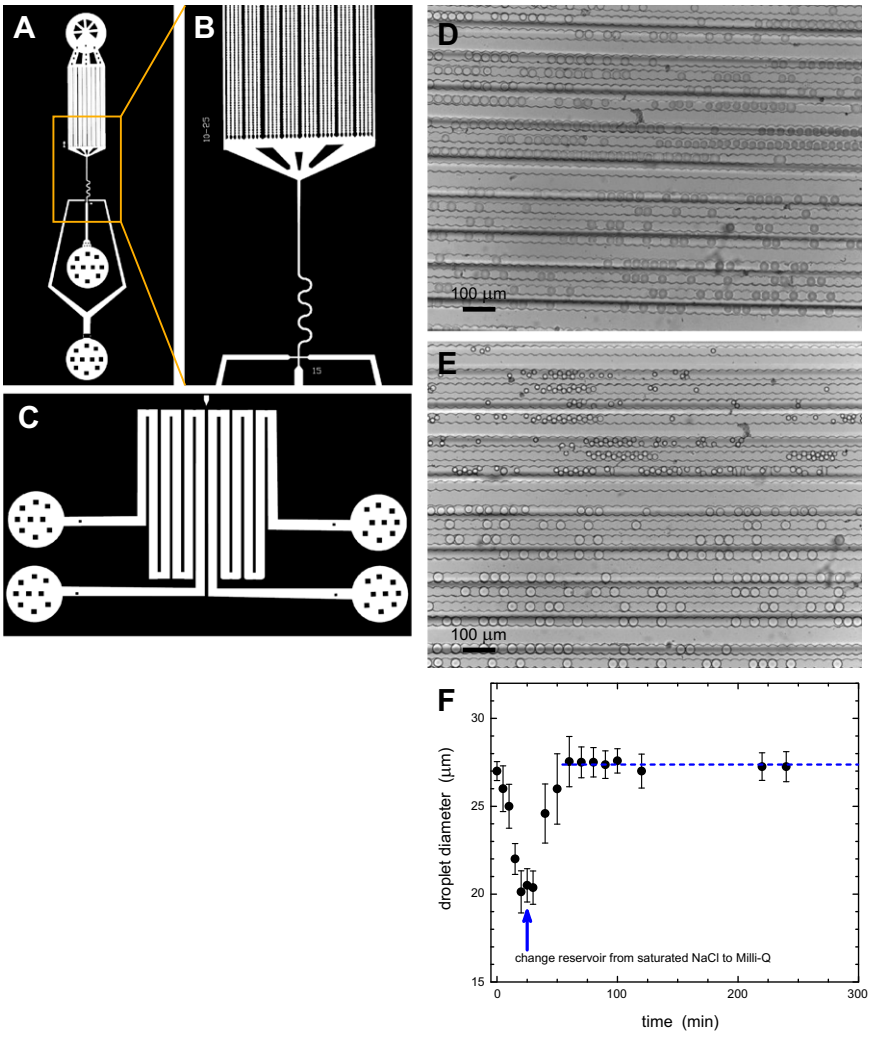

Fig. S1. Microfluidic device design and its robustness. (*A*–*C*) AutoCAD design of the microfluidic device: (*A*) drop spot layer, (*B*) zoomed part of the droplet production site, (*C*) osmotic reservoir layer. (*D* and *E*) Simultaneous tracking of dilute droplets and coacervates on the same chip. (*D*) Bright-field image of just formed droplets. (*E*) Bright-field image taken 40 min after droplet production. The top half of the droplet traps in both images is covered with a PDMS layer containing reservoir channels filled with a concentrated salt solution. The bottom half of the droplet traps is covered with a PDMS layer containing reservoir channels filled with Milli-Q. (*F*) Osmotic shrinkage of droplets can be reversed by exchanging the saturated NaCl solution for Milli-Q.

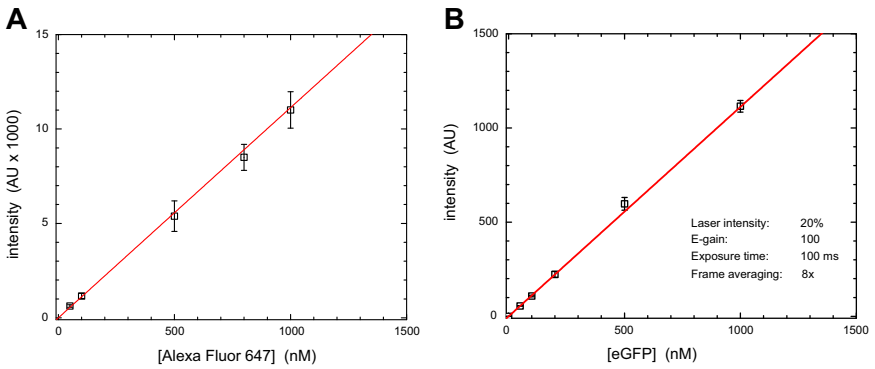

Fig. S2. mRNA and deGFP detection. (*A*) Calibration curve for the molecular beacon using Alexa Fluor 647 (Invitrogen) in droplets. (*B*) Calibration curve of EGFP (Cell Biolabs) in droplets, measured on Olympus IX81 confocal microscope. The detection settings are indicated in the figure.

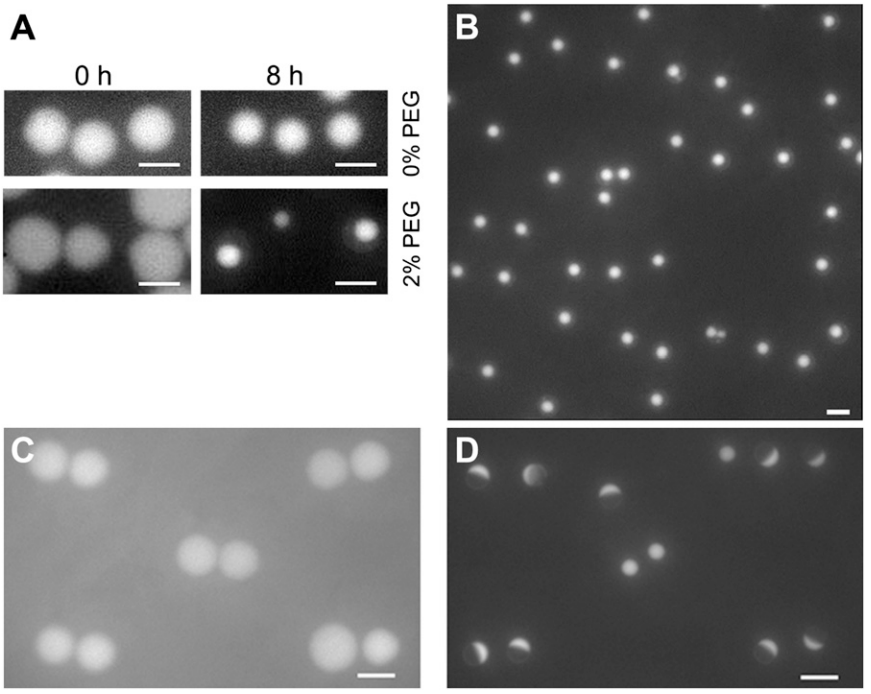

Fig. S3. Phase separation in buffer droplets and cell-free expression mixtures. (*A*) In home-made lysate, we did not observe the emergence of two phases, unless small amounts of PEG 8000 were added, similar to the presence of 2 wt% PEG 8000 in commercial cell-free expression kits. (All scale bars: 20 μm.) (*B*) Phase separation of cell-free expression kit containing lysate and rGFP. (*C* and *D*) Fluorescence microscopy of droplets containing Hepes buffer (100 mM, pH 8.0), 300 mM potassium glutamate, 30 mM magnesium glutamate, 40 g/L PEG 8000, and 0.3 g/L α,ω-di-fluorescein PEG 8000 at $t = 0.00$ h (*C*) and $t = 2.45$ h (*D*). Phase separation of the solution after droplet shrinkage occurred to form a PEG-rich fluorescent phase and a nonfluorescent phase.

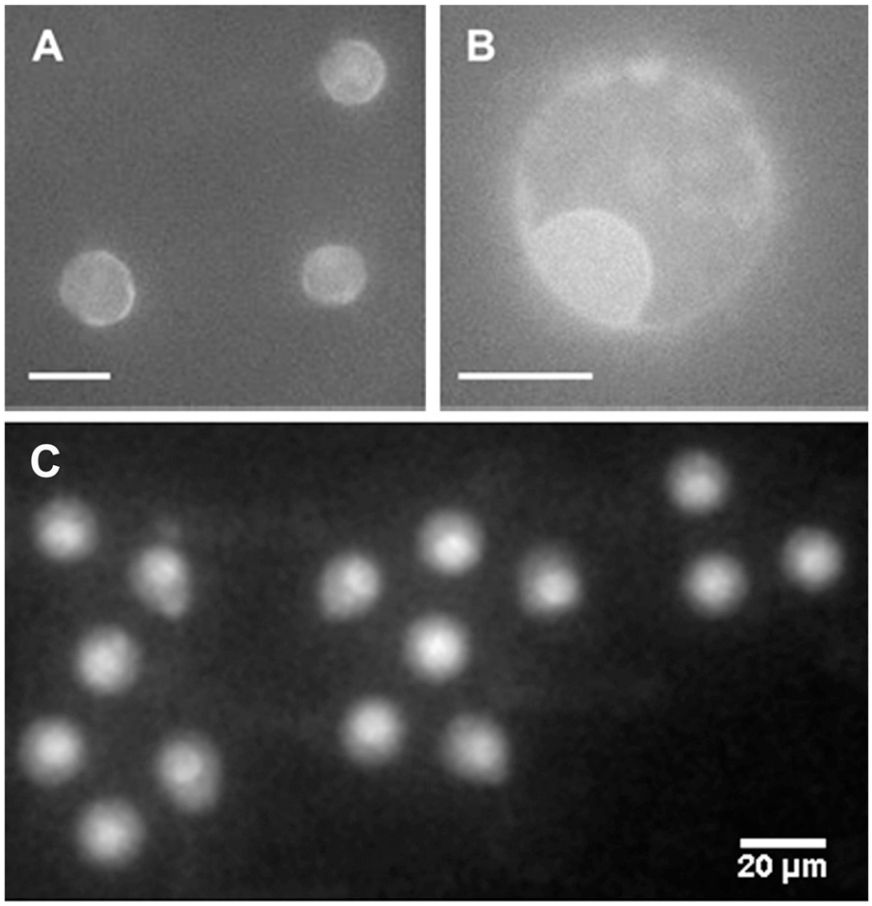

Fig. S4. Partitioning of covalently labeled plasmid DNA. (*A* and *B*) Fluorescence micrographs of fluorescein-labeled plasmid taken at high gain to visualize the adsorption of a fraction of the plasmids to the oil–water interface. (*C*) Fluorescence micrograph of fluorescein-labeled plasmid partitioning in droplets. The image is taken 40 min after initial phase separation. As described in *SI Text*, *S14*, we determined that 46% of all plasmid molecules are localized inside the coacervate phase. A previous study describing plasmid partitioning in PEG two-phase systems is of interest here (1). Image was processed after analysis by adjusting the brightness/contrast and levels in Photoshop CS 5.1. (All scale bars: 20 μm.)

1. Luechau F, Ling TC, Lyddiatt A (2009) Selective partitioning of plasmid DNA and RNA in aqueous two-phase systems by the addition of neutral salt. *Separ Purif Tech* 68(1):114–118.

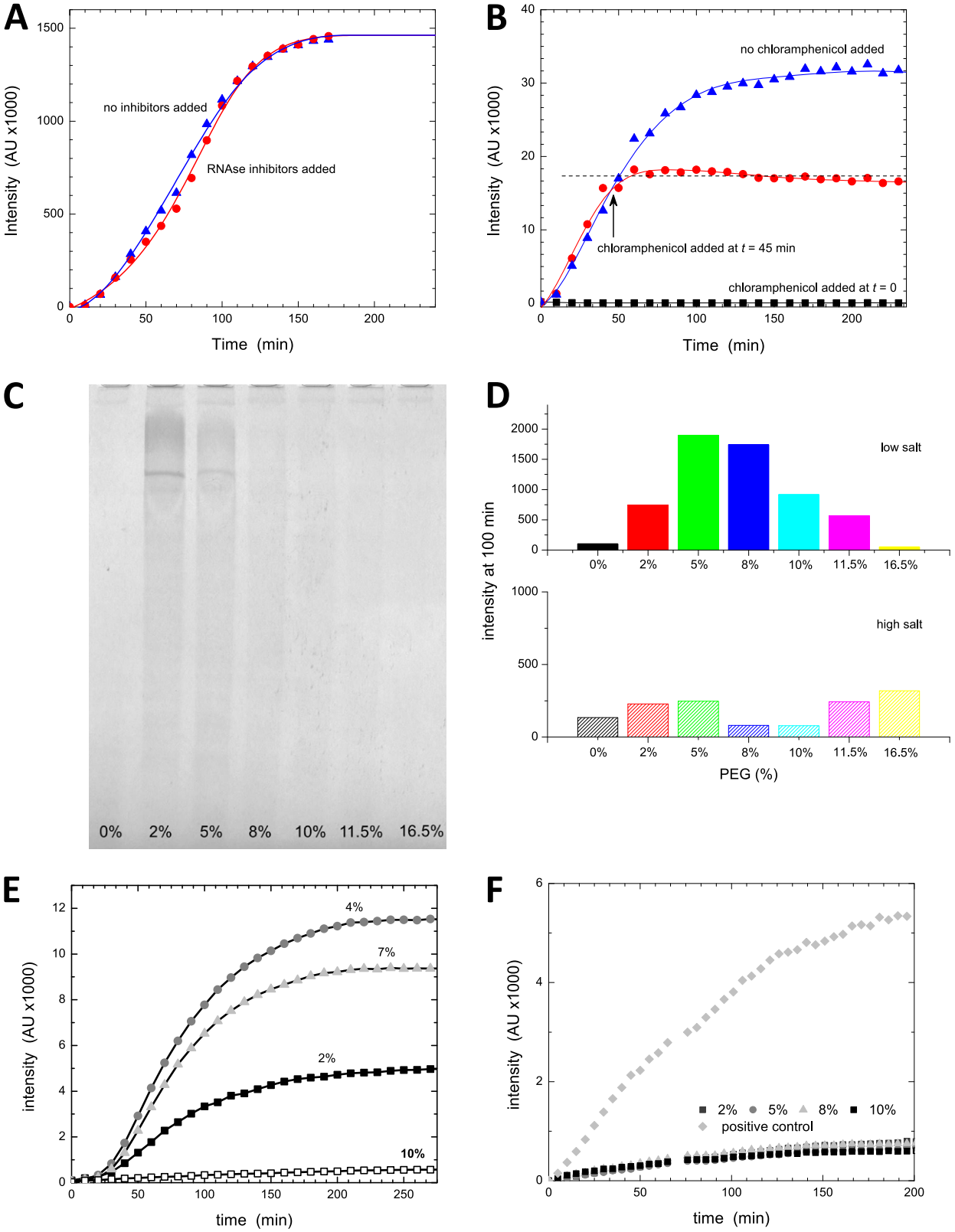

Fig. S5. Control experiments for mRNA and protein degradation over time and inhibition by PEG. (*A*) Addition of RNase inhibitors (Murine; New England Biolabs) to the commercial cell-free expression kit does not change the expression of proteins. mRNA degradation is negligible during the experimental timescales. (*B*) Addition of chloramphenicol to the commercial cell-free expression kit inhibits translation of deGFP. No significant degradation of already formed deGFP is observed on experimental timescales. (*C*) PEG inhibits mRNA transcription at high concentrations. No appreciable mRNA production is observed for PEG concentrations of 8 wt% and above. This observation suggests inhibition of transcription at high PEG concentrations. We note that low concentrations of PEG (up to ~2 wt%) seem to promote transcription, as can been seen by comparing the lanes with 0 wt% and 2 wt% PEG. (*D*) Combination of

Legend continued on following page

high PEG and low and high salt concentrations without compartmentalization into coacervates inhibits mRNA transcription in the same system as used in *C*, and detected by the molecular beacon. DNA concentration in upper panel is 3 nM and in lower panel is 1 nM. (*E*) No appreciable GFP production is observed at 10 wt% PEG, whereas lower PEG concentration shows significant GFP production. This observation suggests inhibition of transcription or translation at high PEG concentrations. (*F*) Combination of high PEG and high salt concentrations without compartmentalization into coacervates inhibits mRNA transcription in the same system as used in Fig. S5*E*. The positive control was measured using a reaction mixture as described in *SI Text*, *S6* with a final concentration of molecular beacon of 1 μM.

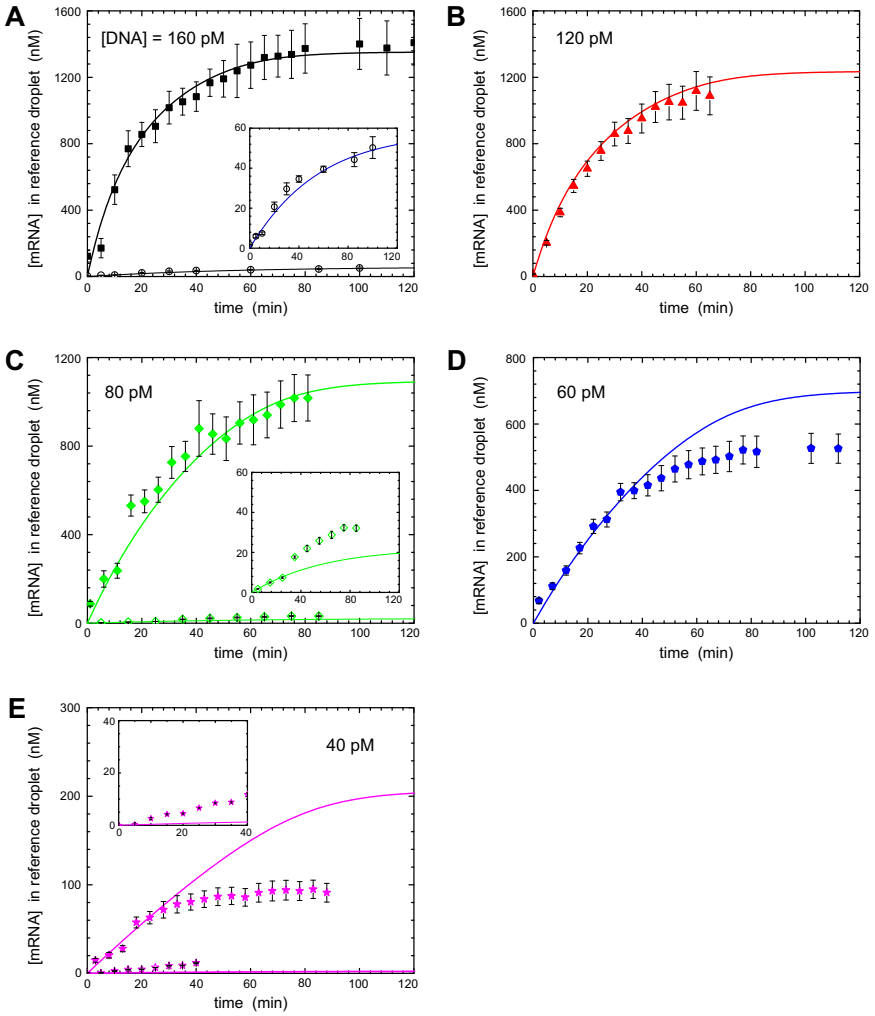

Fig. S6. mRNA production from 40 (*E*), 60 (*D*), 80 (*C*), 120 (*B*), and 160 pM DNA (*A*). The data points represent average concentrations of at least 40 droplets, and the error bars represent their SDs. *Insets* show zoomed part of the data from single-phase droplets. The solid lines are fits of the combined data set to the deterministic model outlined in *SI Text*, *S16*, using the parameters described there. All data points are corrected for the actual size of the droplets (Table S1), and the increased concentrations due to droplet shrinkage. The values shown in this figure are normalized to a reference droplet of 27-μm diameter and a coacervate of 13 μm, respectively, to allow comparison of the different DNA concentrations.

Table S1. Diameters and volume ratios of initial droplets (V_i) and coacervates (V_c) in various experiments

Sample composition	Initial diameter, μm	Shrunk droplet diameter, μm	Coacervate diameter, μm	$K_S = V_i/V_s$	$K_C = V_i/V_c$	Ionic strength at phase separation, M	[PEG] at phase separation, g/L
PEG 8000 in buffer droplets (*SI Text*, *S12*)	24.0 ± 0.20	14.4	14.4 ± 0.39*	4.6	≥9	1.9	180
Fluorescent PEG and lysate (*SI Text*, *S10*)	27.7 ± 0.40	17.3	10.0 ± 0.45	3.7	20	1.9	80
IVTT kit, 160 pM plasmid (*SI Text*, *S6*)	28.5 ± 0.20	20.8	12.4 ± 0.6	2.6	11	1.2	50
IVTT kit, 120 pM plasmid (*SI Text*, *S6*)	25.5 ± 0.4	16.5	10.5 ± 0.45	3.7	13	1.7	70
IVTT kit, 80 pM plasmid (*SI Text*, *S6*)	26.5 ± 1.2	19.5	13.1 ± 0.2	2.5	8	1.2	50
IVTT kit, 60 pM plasmid (*SI Text*, *S6*)	27.5 ± 0.7	20.5	13.0 ± 0.2	2.4	9	1.1	50
IVTT kit, 40 pM plasmid (*SI Text*, *S6*)	26.5 ± 0.6	18.5	11.5 ± 0.5	2.9	12	1.4	60

Internal total salt and PEG concentrations at the moment of coacervate formation were calculated from the volume ratio between initial droplet (V_i) and shrunk droplet at the moment of coacervate formation (V_s) and the known initial ionic strength of the cell-free expression kit, as measured by ICP-OES (*SI Text*, *S13*). IVTT, in vitro transcription and translation.

*Because the shape of the coacervates in this experiment (crescent moon) made an accurate determination of the coacervate volume impossible, we take the coacervates to be hemispheres with a volume equal to half the volume of the shrunk droplet. We note that the volume of these coacervates is not used in any further calculation.

Table S2. ICP-OES analysis of the cell-free expression kit before shrinkage and phase separation, and the coacervates and the dilute phase after phase separation, according to the method described in *SI Text*, *S13*

Element	Concentration before shrinking, mM	Concentration in coacervate, mM	Concentration in dilute phase, mM
K	370	957 ± 136	1,071 ± 172
Na	36	84 ± 15	94 ± 34
Mg	20	22 ± 20	62 ± 20
Zn*	0.01	0.03 ± 0.01	0.04 ± 0.03
P	55	111 ± 41	132 ± 54
S	94	258 ± 33	283 ± 35
K, Na, Mg, Zn combined	426	1,063 ± 171	1,227 ± 226

The average weight of samples before phase separation was 51.7 ± 1.1 mg and after phase separation was 18.7 ± 3.3 mg.

*The Zn signal of all samples was below the detection limit.

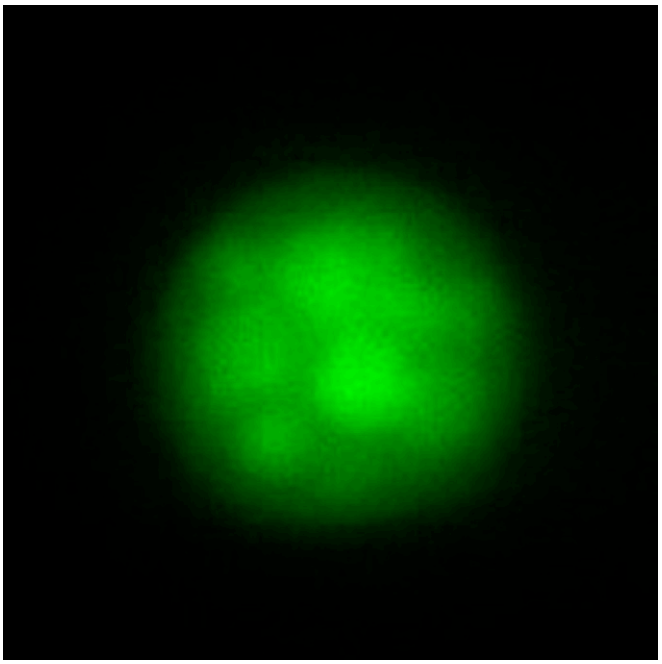

Movie S1. Phase separation of PEG 8000 induced by osmotic shrinkage. False-color fluorescence microscopy movie of fluorescein labeled PEG 8000 in a shrinking microdroplet containing an IVTT mixture prepared as described in *SI Text*, *S10*.

Movie S1